



POLITECNICO
MILANO 1863

RE.PUBLIC@POLIMI

Research Publications at Politecnico di Milano

Post-Print

This is the accepted version of:

S. D'Angelo, D. Vimercati, A. Guardone

A Unified Description of Oblique Waves in Ideal and Non-Ideal Steady Supersonic Flows Around Compressive and Rarefactive Corners

Acta Mechanica, Vol. 229, N. 6, 2018, p. 2585-2595

doi:10.1007/s00707-018-2130-6

This is a post-peer-review, pre-copyedit version of an article published in Acta Mechanica. The final authenticated version is available online at: <https://doi.org/10.1007/s00707-018-2130-6>

Access to the published version may require subscription.

When citing this work, cite the original published paper.

Permanent link to this version

<http://hdl.handle.net/11311/1054367>

A unified description of oblique waves in ideal and non-ideal steady supersonic flows around compressive and rarefactive corners

Stefano D'Angelo · Davide Vimercati · Alberto Guardone

Received: date / Accepted: date

Abstract According to classical gasdynamic theory, if a steady supersonic parallel flow encounters a sudden change in the wall slope, two very different phenomena may possibly occur. If the flow expands around a sharp corner, the well known isentropic Prandtl-Meyer fan is observed. Conversely, a shock wave occurs if the flow is compressed: for wedge angles smaller than the detachment value, which depends on the uniform upstream state, an oblique shock is originated at the corner; at larger deviation angles, a detached shock is formed. A unified description of these flows is presented here to extend the validity of the common $\beta-\vartheta$ (shock angle–deflection angle) diagram for shocked non-isentropic flows into the realm of isentropic expansions. The new graph allows for a straightforward identification of the wave angles for self-similar flow fields around compressive and rarefactive corners. Besides, it clarifies the relation between shock waves and rarefaction fans in the neighbourhood of the $\vartheta = 0$ axis, where shock waves are weak enough to be fairly well approximated by isentropic compressions. At $\vartheta = 0$, indeed, shock and rarefaction curves are demonstrated to be first order continuous. This result is interpreted in view of the bisector rule for oblique shock waves. Exemplary diagrams are reported for both ideal-gas flows, dilute-gas flows and non-ideal flows of dense vapours in the close proximity of the liquid-vapour saturation curve and critical point. The application of the new diagram is illustrated for the textbook case of the supersonic flow past a diamond-shaped airfoil.

1 Introduction

The turning of a uniform steady supersonic flow around a corner is primary to the understanding of compressible-fluid dynamics. In the classical theory of gasdynamics, two main phenomena can possibly occur: shock waves and rarefaction fans (see, e.g., [29]). A shock wave is a sudden compression occurring over a tiny distance of few molecular mean free paths. According to the irreversible nature of the shock phenomenon, the entropy of the fluid increases in passing through the shock wave. On the contrary, a rarefaction fan is an isentropic process consisting in a smooth decompression of the fluid.

Due to their peculiar nature, in the scientific literature shocks and rarefaction fans are often dealt with separately and therefore it is difficult to identify possible similarities between the diagrams depicting these two different phenomena. It is well-known that if the flow deflection is small, the entropy jump across shock waves is negligible [1]. In this isentropic limit, the link between oblique shocks and rarefaction fans can be

Stefano D'Angelo, Davide Vimercati, Alberto Guardone
Department of Aerospace Science and Technology, Politecnico di Milano, Via La Masa 34, 20156 Milano, Italy
E-mail: alberto.guardone@polimi.it

appreciated from the diagrams reporting the value of a thermodynamic quantity downstream of the wave as a function of the deflection angle, for the shock and the fan branches smoothly match (see, e.g., [22]). However, the geometrical properties of the wave pattern around compressive and rarefactive corners have always been treated separately. On one side, the β - ϑ diagram for oblique shock waves provides the slope of an oblique shock β as a function of the deflection angle ϑ . On the other side, the geometrical information regarding the fan configuration is retrieved by the Prandtl-Meyer function. In this work, an extension of the common β - ϑ diagram for oblique shock waves to rarefaction fans is presented, which exemplifies the fundamental similarity between shock and fan waves in the isentropic limit. The new complete diagram requires the definition of a suitable wave angle for centred fans. It is shown that the straightforward choice of the arithmetic mean between the two extreme angles of the fan yields the desired matching with the oblique shock curve. This choice is guided by the bisector rule for oblique shock waves, originally addressed by Kluwick [17] for ideal-gas flows and extended in this work to the non-ideal gas context. The bisector rule indeed states that in the isentropic approximation the shock angle equals the average between the pre-shock and the post-shock characteristic slopes.

Results are presented for both perfect gases, for which the newly introduced diagram depends exclusively on the value of the upstream flow Mach number, and for non-ideal gases, where a marked dependence on the upstream thermodynamic state is also observed and discussed.

The present work is organised as follows. Section 2 reviews the basics of shock waves and rarefaction fans in two-dimensional steady flows. In Sect. 3, the unified description of plane supersonic flows is presented. Application of the extended β - ϑ diagram is illustrated for an exemplary supersonic flow past a diamond-shaped airfoil. Section 4 provides the concluding remarks.

2 Plane supersonic flows around compressive and rarefactive corners

In this section, the theory of oblique shock waves and rarefaction fans is briefly recalled. The present discussion is valid under the assumption that the quantity

$$\Gamma = 1 - \frac{v}{c} \left(\frac{\partial c}{\partial v} \right)_s , \quad (1)$$

where $c = \sqrt{(\partial P / \partial \rho)_s}$ is the speed of sound, is positive. The thermodynamic parameter Γ was named by Thompson [28] as the fundamental derivative of gasdynamics because of its paramount role in delineating the behaviour of compressible fluids. Among the others areas of compressible-fluid dynamics, the fundamental derivative is key in steady isentropic flows (see below), shock wave theory, nozzle flows and non-linear wave propagation [28, 30, 9, 10, 6, 5, 8, 18, 19, 32, 2, 15, 14]. In the references listed above, a distinction is devised between the classical gasdynamic regime if Γ is positive and the non-classical gasdynamic regime if Γ is negative or can possibly change its sign. The latter is so-called because of the unconventional phenomena that characterize it (e.g. rarefaction shocks and composite waves) and it is associated with a sufficiently large level of molecular complexity (e.g. BZT fluids, see also [21, 4, 3]) or to critical-point effects [25, 26]. Within classical gasdynamics, it is also customary to distinguish between the ideal regime if $\Gamma > 1$ and the non-ideal regime if $\Gamma < 1$. The reason for this further distinction is that, whenever $\Gamma > 1$, the flow evolution is qualitatively similar to that of ideal gases with constant specific heats (i.e., perfect gases), for which $\Gamma = (\gamma + 1)/2 > 1$, where γ is the ratio of the specific heats.

In the present work, the discussion is limited to the classical gasdynamic regime. The main implication is that shock waves are compressive, while continuous and smooth fans of acoustic waves are rarefactive. For steady supersonic planar flows, acoustic and shock waves can be either left-running or right-running waves with respect to the local flow direction (see, e.g., [33]). For the wedge/ramp problem under consideration, assuming the uniform supersonic stream incoming from the left, left-running shock waves occur for positive

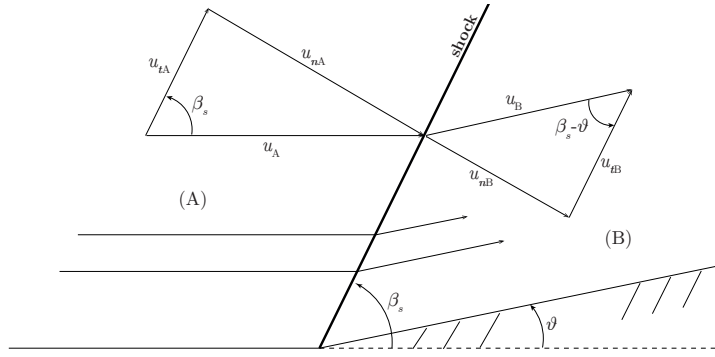


Fig. 1 Oblique shock for streaming flow over a compression corner, where \mathbf{n} is the unit vector normal to the shock front, $u_{\mathbf{n}} = \mathbf{u} \cdot \mathbf{n}$ is the normal velocity (\mathbf{n} is selected such that $u_{\mathbf{n}} > 0$) and $\mathbf{u}_t = \mathbf{u} - u_{\mathbf{n}}\mathbf{n}$ is the tangential velocity. Subscripts A and B indicate the pre-shock and post-shock quantities, respectively.

(counterclockwise) deviation angles, while for negative (clockwise) angles a rarefaction fan appears; the opposite holds for right-running waves.

2.1 Oblique shock wave

Shock waves are thin layers over which an abrupt variation of the thermodynamic and kinematic quantities occur. In the limit of vanishing viscosity and heat conduction, shock waves become surfaces of discontinuity. The balance of mass, momentum and energy across the surface of discontinuity are expressed by the well-known Rankine-Hugoniot relations (see, e.g., Hayes [16]). Let us consider a particular condition about a straight shock front appearing around a wedge or corner, as shown in Fig. 1 for the exemplary case of a left-running shock. The wall prescribes a deviation angle ϑ to the upstream flow, which is realized by a straight shock front originating at the corner and forming an angle β_s with the upstream flow direction. For this configuration, the Rankine-Hugoniot relation can be conveniently recast as

$$[h] = \frac{1}{2}[P](v_A + v_B), \quad (2a)$$

$$-[P]/[v] = (\rho_A \|\mathbf{u}_A\| \sin \beta_s)^2, \quad (2b)$$

$$\rho_A \tan \beta_s = \rho_B \tan(\beta_s - \vartheta), \quad (2c)$$

$$\|\mathbf{u}_A\| \cos \beta_s = \|\mathbf{u}_B\| \cos(\beta_s - \vartheta), \quad (2d)$$

where $[\cdot] = (\cdot)_B - (\cdot)_A$ denotes the jump from the pre-shock state A to the post-shock state B, v is the specific volume, $\rho = 1/v$ is the density, P is the pressure, \mathbf{u} is the fluid velocity, h is the specific enthalpy per unit mass. In particular, one can recognize the Hugoniot relation (2a), which determines the locus of thermodynamic states that can be connected by a shock wave, and the equation of the Rayleigh line (2b), the straight line in $P-v$ plane connecting the pre-shock and post-shock states. Equations (2c) and (2d) enforce the conservation of the mass and of the tangential velocity across the shock front, respectively. Among the solutions of (2), those which are physically admissible must satisfy the entropy condition $s_B - s_A > 0$, where s denotes the specific entropy. It has been shown [1, 31, 13, 22, 24] that in the context of classical gasdynamics

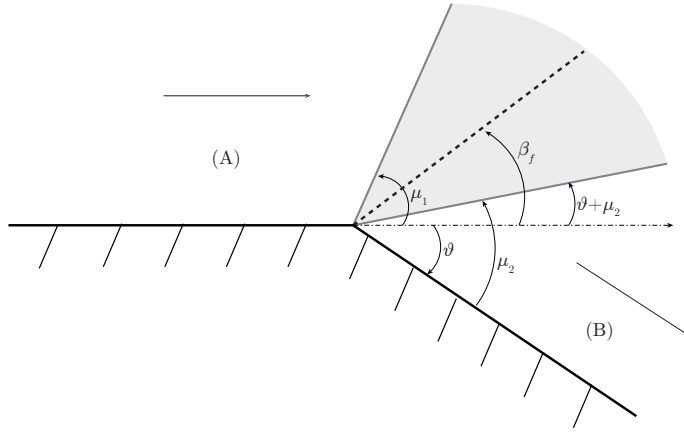


Fig. 2 Centered fan for streaming flow over a refraction corner. The equivalent-fan angle β_f is defined in (5) as the average between the characteristic slopes at the beginning and at the end of the fan.

($\Gamma > 0$), the requirement that entropy is decreasing across the shock wave is sufficient to isolate physically realizable shock solutions¹.

If the pre-shock state A is fixed, for instance by setting P_A , v_A , \mathbf{u}_A , along with the deviation angle ϑ , then, taking into account the equation of state $h = h(P, v)$, system (2) can be solved for the unknowns $(P_B, v_B, \mathbf{u}_B, \beta_s)$, namely the post-shock state and the shock angle. It is well-known that solutions to (2) exist provided that the deviation angle of the stream at the shock wave does not exceed a maximum value ϑ_d , which depends on the pre-shock state [29]. The angle ϑ_d is commonly referred to as the detachment angle because if $|\vartheta| > \vartheta_d$ the turning of the steady supersonic upstream flow is achieved by means of a detached shock wave. For $|\vartheta| < \vartheta_d$, system (2) yields two different solutions, namely the strong oblique shock (larger pressure jump, downstream flow is always subsonic) and the weak oblique shock (lower pressure jump, downstream flow almost always supersonic).

2.2 Rarefaction fan

The turning of a steady supersonic stream around a sharp convex corner is accomplished via a continuous expansion, which occurs in the form of a centred fan (known as rarefaction or Prandtl-Meyer fan) at the corner itself, as shown in Fig. 2 for the exemplary left-running case. In the resulting flow, the entropy and the total enthalpy are both constant, namely $s = \text{cost.}$ and $h^t = h + \|\mathbf{u}\|^2/2 = \text{cost.}$, respectively. From the theory of characteristics (see, e.g., [33]), one obtains

$$\vartheta = \mp(\omega_B - \omega_A), \quad (3)$$

holding for left-running/right-running wave fans, which have slope $\pm\mu$, $\mu = \sin^{-1}(1/M)$, with respect to the local flow direction. In the above expression, subscript A and B indicate the uniform states upstream and downstream the fan, respectively, and ω denotes the Prandtl-Meyer function [7], defined by

$$\omega(\rho; \mathbf{A}) = \omega_r - \int_{\rho_r}^{\rho} \frac{\sqrt{M^2(\rho; \mathbf{A}) - 1}}{M^2(\rho; \mathbf{A})} \frac{d\rho}{\rho}. \quad (4)$$

¹ The shock front can however be neutrally stable to transverse perturbations [11, 20, 12] if the pressure jump is large enough; this kind marginal stability is not discussed in this work.

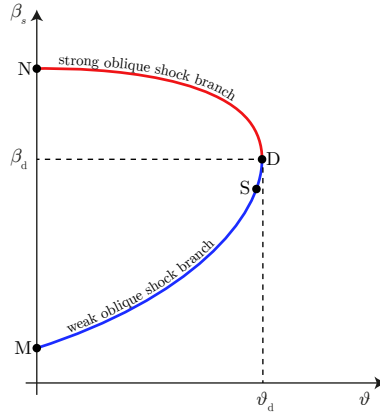


Fig. 3 Qualitative illustration of the β_s - ϑ diagram for left-running oblique shock waves. The shock curve is composed of two branches, namely the weak oblique shock and the strong oblique shock branches, which meet at the detachment point D. Point M indicates the Mach wave limit (no deflection of the flow, vanishing-intensity oblique shock); point N corresponds to the normal shock wave (no deflection of the flow, maximum intensity of the shock wave); point S is the sonic point, at which the downstream Mach number is unitary.

In the above expression, subscript r refers to an arbitrary reference state and the additional parameter \mathbf{A} is a triplet of the form $\mathbf{A} = (P_A, v_A, \mathbf{u}_A)$ indicating the dependence on the upstream state. The parameters \mathbf{A} given above (or any other triplet obtained by straightforward manipulation) determine the constant values of the entropy and of the total enthalpy entering in the definition of the flow Mach number $M(\rho; \mathbf{A}) = \sqrt{2(h^t - h(s, \rho))}/c(s, \rho)$. The Prandtl-Meyer function is often expressed as a function of the of the Mach number (see, e.g., [29,33]); this requires that the Mach number is a monotonic function of the density, which is true at all densities only if $\Gamma > 1$ (for instance, in perfect gases).

Given an upstream state (namely, the triplet \mathbf{A}) and the flow deviation angle ϑ , equation (3) can be solved for the density value ρ_B downstream of the fan. Any other downstream thermodynamic quantities is obtained from the isentropic flow relations and the velocity is retrieved subsequently by enforcing the conservation of the total enthalpy. Moreover, in the particular case in which the Prandtl-Meyer function is monotonically increasing with the Mach number, equation (3) can be solved directly for M_B .

Because of the asymptotic behaviour of the equation of state, the Prandtl-Meyer function attains a finite maximum value ω_{\lim} in the limit $\rho_B \rightarrow 0$ or equivalently $M_B \rightarrow \infty$, i.e. for vacuum conditions at the downstream state. Correspondingly, for any fixed upstream state, the deviation angle has maximal magnitude $\vartheta_v = \mp(\omega_{\lim} - \omega_A)$. Note, however, that at such low densities the continuum theory of gasdynamics cannot be applied and equilibrium isentropic expansion may possibly result in condensation [29].

3 Unified β - ϑ diagram for oblique shocks and rarefaction fans

The geometry of the oblique shock waves is commonly presented in the form of diagrams reporting the oblique shocks angle as a function of the flow deflection angle, namely the β_s - ϑ diagrams, for a number of upstream flow conditions. The general qualitative features of the β_s - ϑ diagram are shown in 3, for the exemplary case of left-running waves. For a given deflection angle, up to the detachment value, two solutions can possibly occur, namely the weak and strong oblique shocks. Therefore, the multivalued function $\beta_s(\vartheta; \mathbf{A})$, in which the dependence on the upstream state is again indicated using the parameter vector \mathbf{A} , is composed by the two branches $\beta_{ws}(\vartheta; \mathbf{A})$ and $\beta_{ss}(\vartheta; \mathbf{A})$ representing the weak and the strong oblique shock solutions,

respectively. Each of these branches is obtained by inverting the relation $\vartheta = \vartheta(\beta_s; \mathbf{A})$, implicitly defined by system (2), in the appropriate range of shock angles, namely in the interval $\beta_s \in [\mu_A, \beta_d]$ for the weak shock branch and in $\beta_s \in [\beta_d, \pi/2]$ for the strong shock branch, where β_d is the shock angle corresponding to the detachment condition.

In the following, a corresponding negative half-plane (considering left-running waves) for rarefaction waves is constructed. The possibility of describing also the rarefaction half-plane would allow for an easier, more versatile and complete diagram than existing ones. To this purpose, we need to define a symmetry between the two governing relations. Thus, an angle β_f which is the counterpart of the β_s angle of oblique shocks, must be introduced for the rarefaction fan. Similarly to the case of oblique shocks, the angle β_f indicates the direction of the fan with respect to the upstream flow.

The natural choice for β_f , justified below by resorting to the bisector rule, is to average the leading characteristic slope $\pm\mu_A$ and the terminating characteristic slope $\vartheta \pm \mu_B$, both computed with respect to the upstream flow direction, namely

$$\beta_f = \frac{\vartheta \pm (\mu_A + \mu_B)}{2}, \quad (5)$$

where the plus/minus sign holds for oblique shocks and rarefaction fans in the left-running/right-running characteristic field, respectively. It is therefore possible to draw a rarefaction fan branch starting at $(0, \pm\mu_A)$ up to the limit condition $(\vartheta_v, (\vartheta_v \pm \mu_A)/2)$. We define a generalized wave angle β , representing either the oblique shock angle or the equivalent fan angle, by introducing the piecewise defined function

$$\beta(\vartheta; \mathbf{A}) = \begin{cases} \beta_s(\vartheta; \mathbf{A}), & \text{if } \pm\vartheta \geq 0, |\vartheta| \leq |\vartheta_d(\mathbf{A})| \\ \beta_f(\vartheta; \mathbf{A}), & \text{if } \pm\vartheta \leq 0, |\vartheta| \leq |\vartheta_v(\mathbf{A})| \end{cases} \quad (6)$$

whose graph provides the extended $\beta-\vartheta$ diagram of left-running/right-running waves around a corner, for a given upstream state (note that the right-running wave curve is simply obtained by 180° rotation of the corresponding left-wave curve). As pointed out above, the shock portion $\beta_s(\vartheta; \mathbf{A})$ is multivalued and comprises the branches $\beta_{ws}(\vartheta; \mathbf{A})$ and $\beta_{ss}(\vartheta; \mathbf{A})$ of weak and strong oblique shocks, respectively.

The definition (5) of the equivalent-fan angle allows to smoothly match (to first order in ϑ) the weak oblique shock branch with the newly defined rarefaction fan branch. Indeed, as it is shown in Appendix A, the piecewise function (6) is continuously differentiable at $\vartheta = 0$, where

$$\left. \frac{d\beta_f}{d\vartheta} \right|_{\vartheta=0} = \frac{\Gamma_A}{2} \frac{M_A^2}{M_A^2 - 1} = \left. \frac{d\beta_{ws}}{d\vartheta} \right|_{\vartheta=0}. \quad (7)$$

The C^1 continuity of the function defined by (6) can be conveniently interpreted in view of the bisector rule for oblique shock waves (see Kluwick [17] and Appendix B), which states that in the isentropic shock limit ($\vartheta \rightarrow 0$ and $P_B \rightarrow P_A$) the shock angle equals the average between the pre-shock and the post-shock characteristic slopes. In passing through the $\vartheta = 0$ axis from the rarefactive to the compressive side, the characteristics delimiting the rarefaction fan fold, thus forming an oblique shock wave. Accounting for the bisector rule, a sort of symmetry is established between the roles of the characteristic waves in the upstream and downstream states and the corresponding “average” wave (either the equivalent fan wave or the shock wave). Condition (7) implies that, as $\vartheta \rightarrow 0$, the rate at which the characteristic lines delimiting the Pradtl-Meyer fan shrink equals the rate at which the pre-shock and post-shock characteristic lines unfold. The C^2 continuity is instead demonstrated to be not guaranteed in Appendix A.

The unified description of supersonic flows around compressive and rarefactive corners, embodied in the complete $\beta-\vartheta$ diagram for both positive and negative deflection angles, is illustrated in Fig. 4a-b for methane (CH_4) under the perfect-gas assumption ($\gamma = 1.32$). Here, the left and right figures correspond to left-running and right-running waves, respectively. As is well-known, for perfect gases both β_s and β_f are independent of the pre-shock thermodynamic state, leaving the upstream Mach number as the only

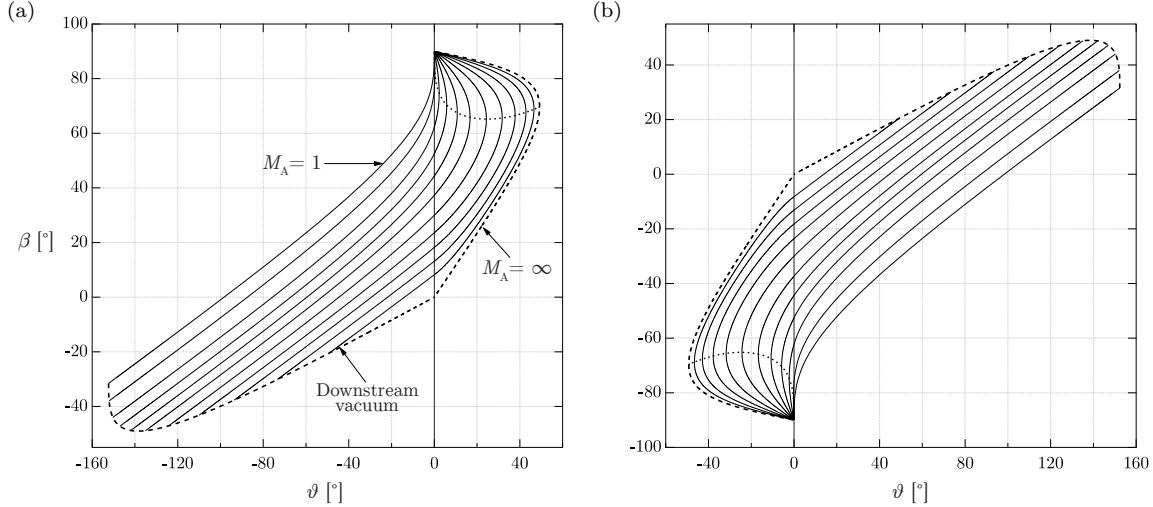


Fig. 4 Extended β - ϑ for (a) left-running and (b) right-running oblique shock waves and rarefaction fans in perfect gas methane. Each curve corresponds to a different upstream Mach number. The limit curve (dashed) is obtained for $M_A = \infty$ on the shock branch and for downstream vacuum conditions on the rarefactive branch. Also shown is the locus (dotted line) of the maximum deviation angles that the fluid can sustain across an attached oblique shock.

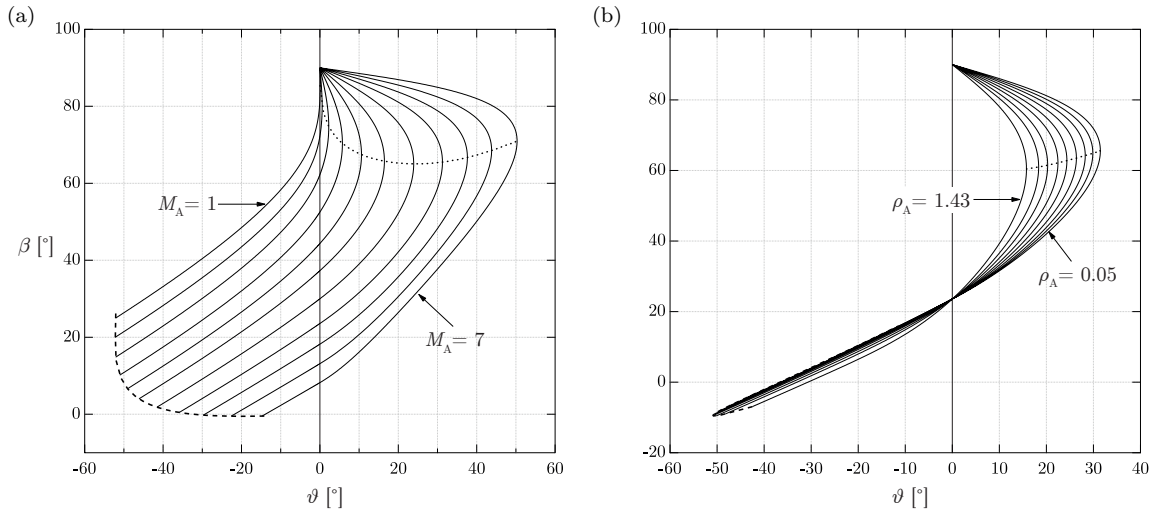


Fig. 5 Extended β - ϑ for oblique shock waves and rarefaction fans in gaseous methane, computed using the well-established thermodynamic library REFPROP. (a) The upstream thermodynamic state is fixed to $P_A = 0.4P_c$, $\rho_A = 0.1\rho_c$; each curve corresponds to a different upstream Mach number. (b) The upstream Mach number is fixed to $M_A = 2.5$; each curve corresponds to a different density along the same isentrope $s_A = s(0.4P_c, 0.1\rho_c)$. For both figures, the rarefaction-fan branch is drawn up to the deviation angle corresponding to downstream saturated conditions (dashed curve). Also shown is the locus (dotted line) of the maximum deviation angles that the fluid can sustain across an attached oblique shock.

Table 1 Fluid properties in each of the uniform states around the diamond-shaped airfoil of Fig. 6, together with the wave angles. The quantities $\vartheta_{i-1,i}$ and $\beta_{i-1,i}$ are the flow deflection angle and the wave angle in passing from state $i - 1$ to state i , respectively, as computed with respect to the upstream flow direction.

Flow region	P/P_c	ρ/ρ_c	M	$\vartheta_{i-1,i} [^\circ]$	$\beta_{i-1,i} [^\circ]$
1	0.4	0.1	2.5	/	/
2	0.29	0.078	2.70	-5	20.15
3	0.062	0.024	3.67	20	8.78
4	0.39	0.083	2.12	26.4	40.45
5	1.56	0.26	1.45	-25	-48.94
6	0.57	0.12	2.12	20	-25.87
7	0.39	0.092	2.35	6.4	-23.45

parameter in the $\beta-\vartheta$ relation. In other words, for a perfect gas, the $\beta-\vartheta-M_A$ representation is independent from the upstream thermodynamic state and therefore it is unique. The dashed curves in Fig. 4a-b represent the limiting cases for both compression and rarefaction waves. In the shock portion, this is obtained for an infinitely large pre-shock Mach number, while, in the rarefaction branch, the limiting curve is the locus of the downstream states corresponding to vacuum conditions.

In contrast with the perfect-gas case, the $\beta-\vartheta$ relation, as computed via any non-ideal equation of state, depends on the choice of the upstream state, as this influences both the shock and the rarefaction curves. Exemplary $\beta-\vartheta$ for gases in non-ideal thermodynamic conditions, namely for sufficiently large upstream densities, are shown in Fig. 5a-b for left-running waves in methane. The fluid is now modelled via the state-of-the-art equation of state described in [27] through the well-established thermodynamic library REFPROP [23]. In Fig. 5a, the upstream thermodynamic state is fixed to $P_A = 0.4P_c$, $\rho_A = 0.1\rho_c$, where subscript c denotes the critical values; each curve thus correspond to a different value of the upstream Mach number. For each case reported, the rarefaction branch extends to the downstream state where condensation occurs (dashed line). On the other hand, in Fig. 5b, the upstream Mach number is fixed to $M_A = 2.5$ and each curve corresponds to a different upstream density value chosen along the same isentrope $s_A = s(0.4P_c, 0.1\rho_c)$. Because the upstream entropy is the same, the rarefactive portions are nearly coincident. It can be noticed that the shock curve is significantly influenced by the value of the pre-shock density. In particular, the maximum deflection angle that the flow can sustain across an attached oblique shock wave is seen to decrease with increasing pre-shock density.

3.1 Example: diamond airfoil in supersonic flight

Ease and versatility of the complete $\beta-\vartheta$ diagram is shown in this section for a typical steady supersonic flow in two dimensions, namely the textbook case of flow past a symmetric diamond-shaped airfoil. Such a case owes both oblique shocks and rarefaction fans for either left- and right-running waves, respectively for the suction and pressure sides. This exemplary configuration is shown in Fig. 6; the fluid considered is, again, methane. The diamond airfoil has a 10° half angle and it is put into a uniform supersonic freestream at an angle of attack of 15° . The freestream conditions are $P_1 = 0.4P_c$, $\rho_1 = 0.1\rho_c$, $M_1 = 2.5$. On the suction surface, the flow is expanded across two rarefaction fans and finally compressed across an oblique shock to match the downstream pressure and flow direction at the slip line emerging from the trailing edge. On the pressure side the flow is initially compressed and subsequently expanded. For each of the wave patterns on the diamond airfoil (except, of course, the contact surface at the trailing edge), the $\beta-\vartheta$ curves obtained from the corresponding upstream state is plotted in Fig. 6, where each wave is also marked. The fluid properties in the different uniform regions around the airfoil are reported in Table 1, together with the flow deviation angles and the wave angles at each corner.

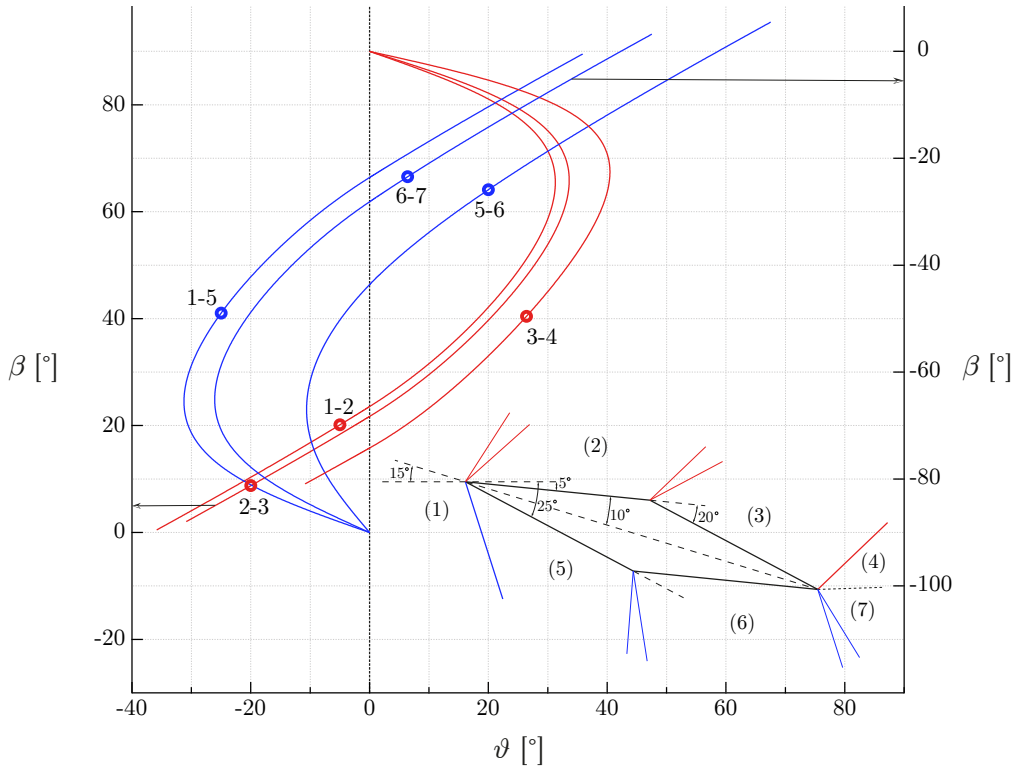


Fig. 6 Complete β - ϑ curves for steady flow of gaseous methane past a diamond-shaped airfoil. The freestream conditions are $P_1 = 0.4P_c$, $\rho_1 = 0.1\rho_c$, $M_1 = 2.5$. The left and right axis are for left-running and right-running waves, respectively. For each of the states upstream of an oblique shock or rarefaction fan, the corresponding β - ϑ curve is drawn and the wave configuration due to flow deflection is marked. Note that the ϑ and β angle refer to the flow direction upstream of each wave pattern. The rarefaction-fan branch is drawn up to the deviation angle corresponding to downstream saturated conditions.

4 Conclusions

A unified approach for the description of the geometrical properties of steady supersonic corner flows in the classical gasdynamic context was presented, which applies to thermally and calorically ideal gases as well as non-ideal fluids. The proposed method took advantage of the definition of an angle β_f for Prandtl-Meyer fans which is equivalent to the angle β_s describing the slope of oblique shocks with respect to the upstream flow direction. Using the newly defined fan angle, the common shock angle-deflection angle diagram for oblique shock waves was extended to deal with centred rarefaction waves. The resulting β - ϑ diagram therefore ranges from the detachment point in the oblique shock portion up to the limiting condition, on the rarefaction side, pointing the expansion into vacuum. The fan angle was chosen to equal the average of the leading and terminating characteristic slopes in the rarefaction fan. This choice was dictated by the analogy between the role of the fan angle thus defined and that of the oblique shock angle in the isentropic limit, whereby the bisector rule states that the oblique shock is the bisector of the characteristic lines delimiting the folded fan. The interplay between the two angles discloses in the C^1 continuity of β - ϑ relation in passing through the no-deviation angle $\vartheta = 0$. Examples of the complete β - ϑ diagram were shown for the perfect-gas case, in which the graph itself is dependent on the value of the upstream Mach

number only, and for non-ideal gases, where a marked dependence on the upstream thermodynamic state is also observed. The new diagram was finally applied to the steady supersonic flow of a non-ideal gas past a diamond-shaped airfoil.

Acknowledgements

The authors thank Prof. Alfred Kluwick for pointing out that the choice of the equivalent fan angle is consistent with the bisector rule and for suggesting to extend the rule to non-ideal fluid flows. This research is supported by ERC Consolidator Grant N. 617603, Project NSHOCK, funded under the FP7-IDEAS-ERC scheme.

A C^1 continuity at $\vartheta = 0$

The functions $\beta_s(\vartheta, A)$ and $\beta_f(\vartheta, A)$ graphed in the two halves of the $\beta-\vartheta$ plane and joining along the vertical axis $\vartheta = 0$ are continuous up to first derivative with respect to ϑ . Of the two shock branches, only the weak shock branch $\beta_{ws}(\vartheta, A)$ will be considered as it is the one adjacent to the rarefaction curve. Continuity up to first order is analytically demonstrated hereunder. For simplicity, the case of left-running shocks and rarefaction fans is considered only; the same results will hold for the right-running counterparts because of rotational symmetry between the $\beta-\vartheta$ relations for left-running and right-running waves. For ease of notation, the dependence of the shock angle function and of the equivalent-fan angle on the upstream state will be omitted. Firstly, if the deviation angle is zero, the oblique shock wave degenerates into an acoustic wave, so that $\beta_{ws}|_{\vartheta=0} = \mu_A$; at the same time, $\beta_f|_{\vartheta=0} = \mu_A$, according to (5). Thus, the piecewise function defined by (6) is continuous at the zero-deviation angle. In order to verify the C^1 continuity at $\vartheta = 0$, the derivatives of the shock angle and its equivalent fan angle are compared. By differentiating (2c), one obtains

$$\frac{d\beta_{ws}}{d\vartheta}\Big|_{\vartheta=0} = -(1 + \tan \mu_A) \left(\rho_A \tan \mu_A + \frac{dv_B}{d\beta_s}\Big|_{\beta_s=\mu_A} \right)^{-1}, \quad (8)$$

in which $\tan \mu_A = 1/\sqrt{M_A^2 - 1}$ and the specific volume derivative with respect to the shock angle, in the acoustic limit, is given by

$$\frac{dv_B}{d\beta_s}\Big|_{\beta_s=\mu_A} = -2 \frac{\sqrt{M_A^2 - 1}}{\rho_A \Gamma_A}. \quad (9)$$

Upon substitution, one gets

$$\frac{d\beta_{ws}}{d\vartheta}\Big|_{\vartheta=0} = \frac{\Gamma_A}{2} \frac{M_A^2}{M_A^2 - 1}. \quad (10)$$

For the equivalent-fan angle, the derivative of β_f with respect to ϑ is simply

$$\frac{d\beta_f}{d\vartheta} = \frac{1}{2} \left(1 + \frac{d\mu_B}{M_B} \frac{dM_B}{d\vartheta} \right), \quad (11)$$

where $d\mu_B/dM_B = -(M_B \sqrt{1 - M_B^2})^{-1}$ and, from the theory of characteristics,

$$\frac{dM_B}{d\vartheta} = -\frac{M_B(1 + (\Gamma_B - 1)M_B^2)}{\sqrt{M_B^2 - 1}}. \quad (12)$$

Substitution in (11) yields, after evaluation at $\vartheta = 0$,

$$\frac{d\beta_f}{d\vartheta}\Big|_{\vartheta=0} = \frac{\Gamma_A}{2} \frac{M_A^2}{M_A^2 - 1}, \quad (13)$$

thus demonstrating, together with (10), the C^1 continuity of the piecewise function defined by (6) at the zero-deviation angle.

By further differentiation, it can be shown that C^2 continuity is not satisfied at $\vartheta = 0$. The long calculations leading to this result for a general equation of state are not presented here. We report, as an example, the expression pertaining the perfect-gas case, which reads

$$\frac{d^2\beta_{ws}}{d\vartheta^2} \Big|_{\vartheta=0} = \frac{d^2\beta_f}{d\vartheta^2} \Big|_{\vartheta=0} + \frac{(\gamma+1)^2}{16} \frac{M_A^4(M_A^2-2)}{(M_A^2-1)^{5/2}}. \quad (14)$$

The above equation shows that for a perfect gas, unless $M_A = \sqrt{2}$, a finite jump in the second derivative exists in passing through the no-deviation condition.

B Bisector rule for steady oblique shock waves

In the neighbourhood of the $\vartheta = 0$ axis, oblique shock waves are weak enough to be well approximated by isentropic compressions. In this limit, the bisector rule states that the slope of an oblique shock equals the average between the pre-shock and post-shock characteristic slopes. The bisector rule, which was originally addressed by Kluwick [17] for the case of perfect gases, is extended here to non-ideal equations of state in the context of classical gasdynamics $\Gamma > 0$. For simplicity, the case of left-running shocks and rarefaction fans is considered only. Using (10) with $\Gamma_A \neq 0$, the Taylor series expansion of the shock angle, in the neighbourhood of $\vartheta = 0$, reads

$$\beta_s = \sin^{-1}(1/M_A) + \frac{\Gamma_A}{2} \frac{M_A^2}{M_A^2 - 1} \vartheta + \mathcal{O}(\vartheta^2), \quad (15)$$

where both angles are measured with respect to the pre-shock flow direction. In the above expression, $\beta_A = \sin^{-1}(1/M_A)$ is the slope of the pre-shock characteristics lines, again with respect to the pre-shock flow direction. The slope of characteristics lines in the post-shock state is

$$\beta_B = \vartheta + \sin^{-1}(1/M_B), \quad (16)$$

where the second term is expanded, in the neighbourhood of $\vartheta = 0$, as

$$\sin^{-1}(1/M_B) = \sin^{-1}(1/M_A) - \frac{1}{M_A \sqrt{M_A^2 - 1}} \frac{dM_B}{d\vartheta} \Big|_{\vartheta=0} \vartheta + \mathcal{O}(\vartheta^2). \quad (17)$$

Because of the isentropic limit, the Mach number derivative in the above expression has the same form as in Prandtl-Meyer waves (12), namely

$$\frac{dM_B}{d\vartheta} \Big|_{\vartheta=0} = - \frac{M_A(1+(\Gamma_A-1)M_A^2)}{\sqrt{M_A^2-1}}. \quad (18)$$

Thus, the post-shock characteristic slope in the isentropic limit is given by

$$\beta_B = \sin^{-1}(1/M_A) + \Gamma_A \frac{M_A^2}{M_A^2 - 1} \vartheta + \mathcal{O}(\vartheta^2), \quad (19)$$

showing that, if oblique shock waves are weak enough that the isentropic approximation applies, namely in the neighbourhood of $\vartheta = 0$,

$$(\beta_A + \beta_B)/2 = \sin^{-1}(1/M_A) + \frac{\Gamma_A}{2} \frac{M_A^2}{M_A^2 - 1} \vartheta + \mathcal{O}(\vartheta^2) = \beta_s, \quad (20)$$

that is, the shock angle is the bisector of the pre-shock and post-shock characteristic lines.

References

1. Bethe, H.A.: The theory of shock waves for an arbitrary equation of state. Technical paper 545, Office Sci. Res. & Dev. (1942)
2. Colonna, P., Guardone, A.: Molecular interpretation of nonclassical gasdynamics of dense vapors under the van der Waals model. *Phys. Fluids* **18**(5), 056,101–14 (2006)
3. Colonna, P., Guardone, A., Nannan, N.R.: Siloxanes: a new class of candidate Bethe-Zel'dovich-Thompson fluids. *Phys. Fluids* **19**(10), 086,102–12 (2007)

4. Cramer, M.S.: Negative nonlinearity in selected fluorocarbons. *Phys. Fluids A* **1**(11), 1894–1897 (1989)
5. Cramer, M.S.: Nonclassical dynamics of classical gases. In: A. Kluwick (ed.) *Nonlinear Waves in Real Fluids*, pp. 91–145. Springer-Verlag, New York, NY (1991)
6. Cramer, M.S., Best, L.M.: Steady, isentropic flows of dense gases. *Phys. Fluids A* **3**(4), 219–226 (1991)
7. Cramer, M.S., Crickenberger, A.B.: Prandtl-Meyer function for dense gases. *AIAA Journal* **30**(2), 561–564 (1992)
8. Cramer, M.S., Fry, N.R.: Nozzle flows of dense gases. *Phys. Fluids A* **5**(5), 1246–1259 (1993)
9. Cramer, M.S., Kluwick, A.: On the propagation of waves exhibiting both positive and negative nonlinearity. *J. Fluid Mech.* **142**, 9–37 (1984)
10. Cramer, M.S., Sen, R.: Shock formation in fluids having embedded regions of negative nonlinearity. *Phys. Fluids* **29**, 2181–2191 (1986)
11. D'yakov, S.P.: On the stability of shock waves. *Zh. Eksp. Teor. Fiz.* **27**(3), 288–295 (1954)
12. Fowles, G.R.: Stimulated and spontaneous emission of acoustic waves from shock fronts. *Phys. Fluids* **24**(2), 220–227 (1981)
13. Gilbarg, D.: The existence and limit behavior of the one-dimensional shock layer. *Am. J. Math.* **73**(2), 256–274 (1951)
14. Guardone, A., Vimercati, D.: Exact solutions to non-classical steady nozzle flows of bethe-zel'dovich-thompson fluids. *J. Fluid Mech.* **800**, 278–306 (2016)
15. Guardone, A., Zamfirescu, C., Colonna, P.: Maximum intensity of rarefaction shock waves for dense gases. *J. Fluid Mech.* **642**, 127–146 (2010)
16. Hayes, W.D.: The basic theory of gasdynamic discontinuities. In: H.W. Emmons (ed.) *Fundamentals of gasdynamics, High speed aerodynamics and jet propulsion*, vol. 3, pp. 416–481. Princeton University Press, Princeton, N.J. (1958)
17. Kluwick, A.: Zur ausbreitung schwacher stöße in dreidimensionalen instationären strömungen. *ZAMM* **51**(3), 225–232 (1971)
18. Kluwick, A.: Transonic nozzle flow of dense gases. *J. Fluid Mech.* **247**, 661–688 (1993)
19. Kluwick, A.: *Handbook of Shock Waves*, chap. 3.4. Rarefaction shocks, pp. 339–411. Academic Press (2001)
20. Kontorovich, V.M.: Concerning the stability of shock waves. *Soviet Phys. JETP* **6** (1958)
21. Lambrakis, K.C., Thompson, P.A.: Existence of real fluids with a negative fundamental derivative Γ . *Phys. Fluids* **15**(5), 933–935 (1972)
22. Landau, L.D., Lifshitz, E.M.: *Fluid mechanics*, 2nd edn. Pergamon Press (1987)
23. Lemmon, E.W., Huber, M.L., McLinden, M.O.: NIST reference database 23: reference fluid thermodynamic and transport properties–REFPROP, version 9.1. Standard Reference Data Program (2013)
24. Menikoff, R., Plohr, B.J.: The Riemann problem for fluid flow of real material. *Rev. Mod. Phys.* **61**(1), 75–130 (1989)
25. Nannan, N.R., Guardone, A., Colonna, P.: Critical point anomalies include expansion shock waves. *Phys. Fluids* **26**(2), 021,701 (2014)
26. Nannan, N.R., Sirianni, C., Mathijssen, T., Guardone, A., Colonna, P.: The admissibility domain of rarefaction shock waves in the near-critical vapour–liquid equilibrium region of pure typical fluids. *J. of Fluid Mech.* **795**, 241–261 (2016)
27. Setzmann, U., Wagner, W.: A new equation of state and tables of thermodynamic properties for methane covering the range from the melting line to 625 k at pressures up to 100 mpa. *J. Phys. Chem. Ref. Data* **20**(6), 1061–1155 (1991)
28. Thompson, P.A.: A fundamental derivative in gasdynamics. *Phys. Fluids* **14**(9), 1843–1849 (1971)
29. Thompson, P.A.: *Compressible Fluid Dynamics*. McGraw-Hill (1988)
30. Thompson, P.A., Lambrakis, K.C.: Negative shock waves. *J. Fluid Mech.* **60**, 187–208 (1973)
31. Weyl, H.: Shock waves in arbitrary fluids. *Comm. Pure Appl. Math.* **2**(2-3), 103–122 (1949)
32. Zamfirescu, C., Guardone, A., Colonna, P.: Admissibility region for rarefaction shock waves in dense gases. *J. Fluid Mech.* **599**, 363–381 (2008)
33. Zucrow, M.J., Hoffman, J.D.: *Gas dynamics*. New York: Wiley, 1976 (1976)